



Derivation of a new set of force field parameters for ammine complexes of chromium(III) containing halogenido ligands: modeling of the *trans*-influence of halogenido ligands

IVANA DJORDJEVIĆ¹, SONJA GRUBIŠIĆ^{1*}, MILOŠ MILČIĆ²
and SVETOZAR NIKETIĆ¹

¹Center for Chemistry, ICTM, University of Belgrade, Njegoševa 12, 11001 Belgrade,
Serbia and ²Faculty of Chemistry, University of Belgrade, Studentski trg 16,
11001 Belgrade, Serbia

(Received 3 September, revised 26 October, accepted 27 October 2014)

Abstract: An approach to model the *trans*-influence using partial atomic charges derived from the molecular electrostatic potential by means of the restrained electrostatic potential (RESP) fitting method is exemplified on a series of halogenido–ammine octahedral chromium(III) complexes. RESP charges incorporated in the present vibrationally optimized consistent force field account for second-order phenomena, improve the modeling and assignment of skeletal vibrations, and reproduce the trends in frequency shifts along the F, Cl, Br, I series. In addition, a supplementary statistical analysis is given for the Cr–halogen bonds in the crystal structures from the CSD.

Keywords: partial atomic charges; chromium(III) complexes; *trans*-influence; consistent force field; skeletal vibrations.

INTRODUCTION

Elucidating structures and properties of chemical species by computational methods has been a growing, fruitful and helpful research practice ever since the emergence of computational chemistry. Essentially two complementary paradigms were developed in previous decades: one stemming from the study of electronic structure based on the first principles of quantum mechanics (QM) and its methods, and the other based on modeling the molecular potential energy surface with empirically derived analytic functions together with a set of adjustable parameters – known collectively as a force field (FF).

An example of synergy between the two paradigms was actualized in the development of an improved and physically more realistic treatment of atomic charges in a force field based on the monopole approximation, by fitting the

*Corresponding author. E-mail: grubisic@chem.bg.ac.rs
doi: 10.2298/JSC030914105D

charges to the QM-derived molecular electrostatic potential. In this context, it was recently shown¹ that atomic charges derived using the restrained electrostatic potential (RESP) program^{2–4} constitute a convenient choice for the optimization of a new generation force field for chromium(III) complexes, which attempts to overcome the limitations of the predefined (*i.e.*, atom-type pre-assigned) atom-centered charges by taking into account the molecular environment of the atoms. (In what follows, the label RESP denotes the computer program of the same name irrespective of whether or not the restraint function is used). For example, the RESP scheme allows each nitrogen ligator atom in $[\text{Cr}(\text{NH}_3)_5\text{X}]^{2+}$ to attain a charge that depends on the arrangement of all other ligator atoms, thus taking care of the mutual influences of the ligands (commonly referred to as *trans-* or *cis*-influences^{5,6}) in the octahedral coordination sphere. The latter phenomena are seldom touched upon in present-day molecular modeling, with the notable exceptions of the comprehensive studies from the Deeth group on Werner-type complexes,⁷ and from Meuwly *et al.* on organometallics.⁸ The atomic point-charge assignment procedure presented in this work (or its potential extensions) could provide another possible way to address the *trans*-influence in a straightforward and simple manner.

Whereas previously basis sets of various complexity were investigated in QM computation of the molecular electrostatic potential (MEP) for $[\text{Cr}(\text{NH}_3)_{6-n}(\text{Cl})_n]^{(3-n)+}$ complexes ($n = 0, 1, 2, 3$),¹ as well as the effect of restraint weighted RESP charges,^{4,9} in this work, QM derived atomic charges were applied in consistent force field (CFF) calculations on $[\text{Cr}(\text{NH}_3)_5\text{X}]^{2+}$ species ($\text{X} = \text{F}, \text{Cl}, \text{Br}, \text{I}$) in order to validate the applicability of the RESP approach for different halogenido ligands, to gauge the anticipated *trans*-influence of X along the halogen series, and to ascertain whether the RESP-derived charges for halogens can reproduce the experimental vibrational frequencies within the vibrationally optimized force field (VOFF) for coordination compounds.¹⁰

METHODOLOGY

All QM computations of MEP were realized using the GAMESS electronic structure program.¹¹ Following former¹ guidelines to avoid the influence of the basis set on the computed MEP values and the RESP-derived partial atomic charges, the restricted open Hartree–Fock (ROHF) method with three out of 12 previously explored basis sets, *i.e.*, the triple- ζ valence basis (TZV),¹² the effective core potential valence basis (SBKJC),^{13,14} and the Dunning-type correlation consistent basis set with polarization function (cc-pVTZ),¹⁵ was used for the metal ion. The three basis sets produced practically the same final results for the optimized geometries and vibrational frequencies. For all other atoms, the following were employed: the 6-31G(d) polarized basis set¹⁶ for N, F, and Cl atoms, the 6-311G(d) basis^{17,18} for Br and I atoms, and the unpolarized Pople 6-31G basis set¹⁹ for the ammine H atoms. This choice of the computational level offered the best compromise between feasibility of the procedures, the consistency of the results, and computational economy.

The RESP program⁴ to derive partial atomic charges from MEP was used as set out previously.¹ Atomic charges were fitted iteratively⁹ and a satisfactory convergence was achieved in all cases (the residual sum of squares, χ^2 , below 0.007 and the standard error of estimate, χ^2/n , below 0.003). Departure from the HF/6-31G*, traditionally employed in RESP procedures, was both possible and necessary in order to obtain physically realistic and consistent results, and was paralleled in other similar improvements of RESP strategies (*e.g.*, within AMBER^{20,21} or CHARMM²² schemes) in the last decade.

Force field calculations and the analysis of normal vibrations were performed with the consistent force field (CFF) program for transition metal complexes and VOFF.¹⁰ Additional force field parameters related to halogeno atoms were introduced as required and the values are given in Table S-I of the Supplementary material to this paper. The parameters were systematically derived to archive the closest possible match of calculated and experimental stretching vibrations. The details and the components of the force field (potential functions for bond stretching, angle bending, torsional, non-bonded and electrostatic contributions) were particularized earlier.¹⁰

All geometry optimizations (energy minimizations) were performed using the Newton–Raphson analytical second derivatives method. The root mean squared deviation of the gradient at convergence was always $<10^{-7}$ kcal mol⁻¹ Å⁻¹, and the experimental crystal structures were reproduced with an average deviation of 0.005 Å in the bond lengths and 0.5° in the bond angles.

Supporting density functional theory (DFT) computations (*cf.* Subsection: Modeling the *trans*-influence of X) were performed using Gaussian09,²³ with either the hybrid B3LYP functional,^{24,25} the standard LANL2DZ-ECP basis²⁶ for Cr and I atoms, and 6-31G(d,p) basis¹⁹ for H, N, C, F, Br and Cl atoms, or the S-VWN functional^{27–29} with 6-31+G(d) basis¹⁶ for all atoms. Geometries of [Cr(NH₃)₅X]²⁺ were optimized without any symmetry restrictions in the gas phase and the minima were confirmed by frequency calculations.

RESULTS AND DISCUSSION

Crystal structures

A search for structural data on [Cr(NH₃)_{6-n}(X)_n]⁽³⁻ⁿ⁾⁺ (X = F, Cl, Br, I) revealed only a modest number of published reports on their crystal structures, which prevented any value for the equilibrium metal–ligand (M–L) bond lengths to be inferred from, *e.g.*, a statistical distribution of the observed M–L distances. Angular deformations of octahedra were sufficiently small and/or induced externally, enabling the adoption of the values $\pi/2$ and π for the reference valence angle parameters in the force field for metal centers throughout this study.

Furthermore, since the only one complete series of experimentally characterized structures, namely the one with $n = 1$, is available, the present discussion will be restricted to the [Cr(NH₃)₅X]²⁺ (X = F, Cl, Br, I) series. CFF modeling of the other series (with two or more coordinated halogenido ligands) did not reveal any new features, but corroborated all the findings presented herein.

Standard bond lengths were sought in the 1989 compilation³⁰ of the data from the Cambridge structural database (CSD) as apparently no updates were published in the meantime. The values relevant for this work (Table I; part A)

show that the number of Cr–X bonds characterized experimentally are mainly insufficient. However, taking into consideration all the crystal structures published after the issuing of the 1989 tables,³⁰ it was possible to generate more reliable statistic (see Table I; part B). For 124 Cr–F bonds, there were 12 outliers from two structures (occurring at $> 4\sigma$), and another two were eliminated on chemical criteria. For 120 Cr–Cl bonds, only five distances were eliminated on chemical criteria. In both cases, the remaining values represented acceptably unimodal distributions. For 30 Cr–Br bonds, the distribution of values appeared to be bimodal, but an elimination of 6 values from a total of two structures did decrease the standard deviation appreciably, so a further reduction was not considered necessary for the present purpose. The number of Cr–I bonds was still too low, but the values were grouped in two narrow intervals, one of which (with the longer bond lengths) was eliminated on chemical grounds. Distribution of all Cr–X bonds is presented as bar diagrams in Fig. S-1 of the Supplementary material.

TABLE I Metal–ligand bond lengths (Å) from X-ray diffraction data for octahedral chromium(III) complexes given as: unweighted mean (d), median (m), standard deviation (σ), lower quartile (q_L), upper quartile (q_U), and the number of observations (n)

Bond	d	m	σ	q_L	q_U	n	Excl. ^a
A. Data from CSD (1989) ^b							
Cr–F	1.870	1.872	0.027	1.847	1.892	5	–
Cr–Cl	2.335	2.318	0.055	2.303	2.370	9	–
	2.309	2.316	0.018	2.229	2.319	7	–
Cr–Br	2.577	–	–	–	–	1	–
Cr–I	2.669	–	–	–	–	1	–
	2.781	–	–	–	–	1	–
B. Data from CSD (2013) ^c							
Cr–F	1.881	1.882	0.024	1.812	1.960	112	12,(2)
	1.882	1.883	0.023	1.841	1.960	110	2,(2)
Cr–Cl	2.325	2.322	0.022	2.287	2.389	120	–
	2.323	2.322	0.018	2.287	2.372	115	5,(3)
Cr–Br	2.481	2.479	0.025	2.436	2.521	28	2,(1)
	2.471	2.470	0.018	2.436	2.502	24	4,(1)
Cr–I	2.687	2.662	0.044	2.648	2.750	7	–
	2.662	2.662	0.010	2.648	2.677	5	2,(1)

^aValues shown: excluded Cr–X bonds, (excluded structures); ^bquoted from Orpen *et al.*;³⁰ ^cCambridge structural database 5.35 (Nov. 2013. + updates)

In keeping with the common practice of CFF,^{31,32} the reference bond-length parameters in the bond stretching potential functions were assigned values which reproduce, after geometry optimization, the mean values of experimental bond lengths – in this case from X-ray diffraction studies, corresponding to r_a values in the Kuchitsu notation.³³ Taking into consideration previous bond stretching

parameters from VOFF,¹⁰ and the mean values of r_α as given in Table I (part B), the following values for reference bond-length parameters were assigned: Cr–F 1.883 Å, Cr–Cl 2.300 Å, Cr–Br 2.400 Å, Cr–I 2.620 Å, Cr–N 2.052 Å, and N–H 0.950 Å. In furtherance of the discussion on the *trans*-influence (see Subsection: Modeling the *trans*-influence of X), it should be emphasized that the reference bond-length parameters, as well as bond-stiffness constants, were identical for all Cr–N bonds.

The coordination polyhedra of all structures were assumed to possess the highest possible symmetry (O_h for CrN_6 , and C_{4v} for CrN_5X), due to the absence of any experimental data that might indicate otherwise.

Atomic charges

The choice of the RESP program and details about its application in the derivation of partial atomic charges from the QM molecular electrostatic potential for octahedral complexes of chromium(III) was already justified.¹ In particular, the selection of the restraint weight,⁹ needed for the treatment of atoms buried inside larger structures, was explored and it was found that the central metal atom does not quite behave as buried, enabling the use of the single-stage derivation mode (*viz.* the “ESP” option) of the RESP program.

The results for $[\text{Cr}(\text{NH}_3)_5\text{X}]^{2+}$ complexes (X = F, Cl, Br, I) are summarized in Table II. General trends reported previously¹ for $[\text{Cr}(\text{NH}_3)_{6-n}(\text{Cl})_n]^{(3-n)+}$ ($n = 0, 1, 2, 3$) complexes are perceived here as expected: for example, a decrease of $q(\text{X})$ is followed by a small decrease of $q(\text{M})$ and a marked decrease of $q(\text{N}^{\text{ax}})$. Furthermore, a comparison of the partial atomic charges with other previously published data (Table S-II of the Supplementary material) shows that trends (*e.g.*, decrease of $q(\text{M})$ upon substitution by X, or decrease of $q(\text{X})$ in the halogen series from F to I) are in full agreement, notwithstanding the differences in the reported values, even in cases when they originate from the same laboratory (Table S-II of the Supplementary material).

TABLE II. RESP atomic charges (esu) for complexes $[\text{Cr}(\text{NH}_3)_5\text{X}]^{2+}$ (X = F, Cl, Br, I), calculated with three different basis sets for the metal atom; q = RESP atomic charges, eq = equatorial or *cis*(X,NH₃), ax = axial or *trans*(X,NH₃), TZV = triple- ζ valence basis, SBKJC = effective core potential valence basis, cc-pVTZ = Dunning-type correlation consistent basis set with polarization function

Basis for Cr(III)	$q(\text{Cr})$	$q(\text{X})$	$q(\text{N})$	$q(\text{H})$
$[\text{Cr}(\text{NH}_3)_5(\text{X})]^{2+}$ (X = F)				
TZV	1.6409	-0.5867	-1.0317 ^{eq} -1.0000 ^{ax}	0.4083 ^{eq} 0.3898 ^{ax}
			-1.0366 ^{eq} -1.0530 ^{ax}	0.4083 ^{eq} 0.4032 ^{ax}
SBKJC	1.6668	-0.5896		

TABLE II. Continued

Basis for Cr(III)	$q(\text{Cr})$	$q(\text{X})$	$q(\text{N})$	$q(\text{H})$
[Cr(NH ₃) ₅ (X)] ²⁺ (X = F)				
cc-pVTZ	1.6340	-0.5941	-1.0128 ^{eq} -1.0718 ^{ax}	0.4046 ^{eq} 0.4091 ^{ax}
[Cr(NH ₃) ₅ (X)] ²⁺ (X = Cl)				
TZV	1.1800	-0.4400	-0.9087 ^{eq} -0.5672 ^{ax}	0.3819 ^{eq} 0.2929 ^{ax}
SBKJC	1.1804	-0.4386	-0.9134 ^{eq} -0.5701 ^{ax}	0.3834 ^{eq} 0.2936 ^{ax}
cc-pVTZ	1.1333	-0.4364	-0.8826 ^{eq} -0.5899 ^{ax}	0.3770 ^{eq} 0.2999 ^{ax}
[Cr(NH ₃) ₅ (X)] ²⁺ (X = Br)				
TZV	0.8217	-0.3420	-0.7925 ^{eq} -0.1928 ^{ax}	0.3558 ^{eq} 0.2044 ^{ax}
SBKJC	0.8032	-0.3350	-0.7917 ^{eq} -0.1791 ^{ax}	0.3561 ^{eq} 0.2013 ^{ax}
cc-pVTZ	0.7739	-0.3394	-0.7682 ^{eq} -0.2037 ^{ax}	0.351 ^{eq} 0.2086 ^{ax}
[Cr(NH ₃) ₅ (X)] ²⁺ (X = I)				
TZV	0.5399	-0.2243	-0.6171 ^{eq} -0.1677 ^{ax}	0.3084 ^{eq} 0.2066 ^{ax}
SBKJC	0.5315	-0.2202	-0.6154 ^{eq} -0.1809 ^{ax}	0.3082 ^{eq} 0.2106 ^{ax}
cc-pVTZ	0.4843	-0.2193	-0.5904 ^{eq} -0.1827 ^{ax}	0.3034 ^{eq} 0.2127 ^{ax}

By default in the CFF program, the atom-centered effective point charges used to evaluate the Coulomb potential are chosen from the table of force field values based on the atom type. However, in this as well as in the previous study,¹ the RESP charges (as given in Table II) were directly assigned to individual atoms together with their atomic coordinates.

Vibrational spectra

For the 22-atom [Cr(NH₃)₅(X)]²⁺ species there are 60 vibrational normal modes, which are classified into $12A_1 + 4A_2 + 7B_1 + 5B_2 + 16E$ in the point group C_{4v} defined by the non-hydrogen (skeletal) atoms of [Cr(NH₃)₅X]²⁺. Symmetry coordinates can be described in terms of the following redundant set of 68 internal coordinates: ΔR_i ($\nu(\text{Cr-L})$, $i = 1,6$; L = N,X), Δr^k_i ($\nu(\text{N-H})$, $i = 1,5$; $k = 1,3$), $\Delta\alpha_{ij}$ ($\delta(\text{L-Cr-L})$, $i = 1,5$; $j = i+1,6$; L = N,X), $\Delta\beta^k_i$ ($\delta(\text{Cr-N-H})$, $i = 1,5$; $k = 1,3$), $\Delta\gamma^k_i$ ($\delta(\text{H-N-H})$, $i = 1,5$; $k = 1,3$), and five torsional angles $\Delta\tau_i$ ($i = 1,5$) defining internal rotation of the ammine ligands about the Cr–N bonds. Eighteen internal coordinates (R,α) define 11 skeletal modes ($4A_1 + 2B_1 + B_2 + 4E$; total degeneracy = 15) of the CrN₅X moiety. The remaining 45 internal coordinates (r ,

β, γ) describe the ammine $\nu(\text{N}-\text{H})$, $\delta(\text{H}-\text{N}-\text{H})$, and $\delta(\text{Cr}-\text{N}-\text{H})$ vibrations. One of the possible ways to label the latter modes in the C_{4v} point group is based on two assumptions: the first, to impose the invariance of the hydrogens on the axial ammine ligand to all symmetry operations in C_{4v} , and the second, to apply the projection operator method onto the basis consisting of orthogonal linear combinations of internals derived from the treatment of ammonia molecule in the C_{3v} point group³⁴ instead of the internals ($\text{N}-\text{H}$, $\text{H}-\text{N}-\text{H}$, and $\text{Cr}-\text{N}-\text{H}$) themselves. In this way, it was possible to obtain the following five sets of symmetry coordinates for $[\text{Cr}(\text{NH}_3)_5\text{X}]^{2+}$ in C_{4v} (with the total degeneracies shown in parentheses): symmetrical $\text{N}-\text{H}$ stretching and symmetrical $\text{H}-\text{N}-\text{H}$ bending (“umbrella”) modes (each spanning $2A_1 + B_1 + E$; (5)), antisymmetrical $\text{N}-\text{H}$ stretching, antisymmetrical $\text{H}-\text{N}-\text{H}$ bending, and NH_3 rocking (sometimes referred to as libration) modes (each spanning $A_1 + A_2 + B_1 + B_2 + 3E$; (10)) totaling to 40 optical modes. The inventory is completed with five torsional modes (transforming as $A_1 + A_2 + B_2 + E$; (5)) derived in the same way. The skeletal modes of CrN_5X and a possible distribution of all normal modes for $[\text{Cr}(\text{NH}_3)_5\text{X}]^{2+}$ in the point group C_{4v} are given in Figure S-2 and Table S-III of the Supplementary material, respectively.

Since the assignments over the entire spectral range are in general accord with the published analyses of vibrational spectra of $[\text{Cr}(\text{NH}_3)_5\text{X}]^{2+}$ species (as shown in Table III), the focus here will be on the shifts of low frequency intramolecular modes in the series F, Cl, Br, I, which was the key question addressed in this paper. The most prominent tendency was an expected decrease in the $\text{Cr}-\text{X}$ stretching frequency with increasing mass of X (see Table IV), which is in full correspondence with the experimental data. Although a further refinement of the VOFF was possible, it was not considered opportune in this case for at least two reasons. First, in line with the consistent force field (CFF) paradigm,^{31,32,37,38} the force field parameters are not equatable to the derived vibrational force constants; hence, their optimization is meaningful only with respect to a wider range of observables for a family of related chemical species. In addition, crystal lattice effects (hydrogen bonds, counter-ion interactions, *etc.*), which are observed in solid-state IR spectra, were not explicitly treated in the present modeling study. Therefore, they are included in the force field parameters in an indirect way, thus obviating the need for additional parameter optimization as long as the differences among experimental values (of vibrational frequencies) are of the same order of magnitude as the differences between experimental and calculated values. Supporting DFT calculations (Subsection: Modeling the *trans*-influence of X) yielded vibrational frequencies (Table S-IV of the Supplementary material) that are in general agreement with those shown in Tables III and IV, except for the $\nu_a(\text{NH}_3)$, which were placed slightly above the experimental values.

TABLE III. Comparison of experimental vibrational frequencies (cm^{-1}) for $[\text{Cr}(\text{NH}_3)_5\text{X}]^{2+}$ ($\text{X} = \text{F}, \text{Cl}, \text{Br}, \text{I}$) to the corresponding values calculated using RESP charges¹ and VOFF parameters¹⁰; key: v = stretching, δ = bending (deformation), ρ = rocking, s = symmetric, a = antisymmetric

Principal assignment	Sym.	X = F		X = Cl		X = Br		X = I	
		Exp. ^a	Calc.	Exp. ^a	Calc.	Exp. ^a	Calc.	Exp. ^a	Calc.
$v_a(\text{NH}_3)$	B_1	—	3277	3277 ^b	3275	—	3277	—	3277
		—	3270	—	3271	—	3270	—	3271
$v_s(\text{NH}_3)$	E	—	3162	—	3160	—	3161	—	3161
		—	3160	—	—	—	—	—	—
$\delta_a(\text{H}-\text{N}-\text{H})$	B_1	—	1627	—	1618	—	1613	—	1611
		—	1589	1600 ^b	1583	—	1587	—	1586
$\delta_s(\text{H}-\text{N}-\text{H})$	E	—	1337	—	1303	—	1323	—	1318
		—	1323	1289 ^b	1293	—	1314	—	1309
$\rho_a(\text{NH}_3)$	B_1	—	748	774 ^b	758	—	765	—	759
		—	710	—	702	—	711	—	700
$v(\text{Cr}-\text{X})$	A_1	540 ^c	534	302 ^d 306 ^e	305	204 ^d 206 ^f	187	184 ^d 195 ^g	177
$v(\text{Cr}-\text{N})$	E	470 ^c	474	472 ^{d,e}	469	474 ^d 470 ^f	470	463 ^d 467 ^g	469
	A_1	462 ^c	439	460 ^d 462 ^e	448	463 ^d 453 ^f	449	457 ^d 454 ^g	450
	A_1	428 ^c	387	433 ^d 434 ^e	407	438 ^f	403	440 ^d 442 ^g	402
	B_1	399 ^c	380	406	371	425 ^d 427 ^f	372	415 ^d 417 ^g	370
$\delta(\text{N}-\text{Cr}-\text{N})$	B_2	—	313	—	296	—	293	—	288
	E	275 ^c	274	285 ^d	281	287 ^d 274 ^f	271	260 ^d 261 ^g	269
	E	260 ^c	257	255 ^{d,e}	266	265 ^d 259 ^f	263	250 ^d 248 ^g	257
	E	238 ^c	235	—	241	250 ^d 248 ^f	244	240 ^d 238 ^g	244
	B_1	—	190	200 ^d	200	—	196	—	196
$\delta(\text{N}-\text{Cr}-\text{X})$	E	214 ^c	217	—	—	—	—	—	—
	E	184 ^c	181	170 ^{d,e}	167	172 ^d 171 ^f	171	172 ^d 168 ^g	163
	E	—	—	124 ^d 126 ^e	127	122 ^{d,f}	128	116 ^d 112 ^g	111
$\delta(\text{N}-\text{Cr}-\text{N})$	E	114 ^c	120	114 ^{d,e}	103	110 114 ^f	117	—	—

^aFrom Schmidtke and Rosner,³⁵ unless otherwise noted; ^bfrom Tanaka *et al.*,³⁶ counter-ions: c = perchlorate, d = nitrate, e = chloride, f = bromide, g = iodide

TABLE IV. Principal assignment of the skeletal vibrations (cm^{-1}) for $[\text{Cr}(\text{NH}_3)_5\text{X}]^{2+}$ ($\text{X} = \text{F}, \text{Cl}, \text{Br}, \text{I}$)

No.	$[\text{Cr}(\text{NH}_3)_5(\text{F})]^{2+}$			$[\text{Cr}(\text{NH}_3)_5(\text{Cl})]^{2+}$			$[\text{Cr}(\text{NH}_3)_5(\text{Br})]^{2+}$			$[\text{Cr}(\text{NH}_3)_5(\text{I})]^{2+}$		
	Sym	PED	v	Sym	PED	v	Sym	PED	v	Sym	PED	v
41	A_1	S_4+S_5	534	A_1	S_4+S_5	305	A_1	S_4+S_5	187	A_1	S_4+S_5	177
42	E	$2S_3$	474	E	$2S_3$	469	E	$2S_3$	470	E	$2S_3$	471
43	E	$2S_3$	473	E	$2S_3$	469	E	$2S_3$	470	E	$2S_3$	470
44	A_1	$S_1+S_4+S_5$	439	A_1	$S_4-S_5-S_8$	448	A_1	$S_4-S_5-S_8$	449	A_1	$S_4-S_5-S_8$	450
45	A_1	$S_1-S_4-S_5$	387	A_1	$S_1-S_4+S_5$	407	A_1	$S_1-S_4+S_5$	403	A_1	$S_1-S_4+S_5$	402
46	B_1	S_2	380	B_1	S_2	371	B_1	S_2	372	B_1	S_2	370
47	B_2	S_6	313	B_2	S_6	296	B_2	S_6	293	A_1	S_8	298
48	E	S_7+S_{11}	289	E	S_7+S_{11}	281	A_1	$S_8+S_4+S_5$	293	B_2	S_6	288
49	E	S_7+S_{11}	274	E	S_7+S_{11}	266	E	S_7+S_{11}	271	E	S_7+S_{11}	269
50	E	S_7+S_{11}	257	E	S_7+S_{11}	241	E	S_7+S_{11}	263	E	S_7+S_{11}	257

TABLE IV. Continued

No.	[Cr(NH ₃) ₅ (F)] ²⁺			[Cr(NH ₃) ₅ (Cl)] ²⁺			[Cr(NH ₃) ₅ (Br)] ²⁺			[Cr(NH ₃) ₅ (I)] ²⁺		
	Sym	PED	ν	Sym	PED	ν	Sym	PED	ν	Sym	PED	ν
51	<i>A</i> ₁	S ₈	248	<i>A</i> ₁	S ₈	226	<i>E</i>	S ₁₀ +S ₁₁	244	<i>E</i>	S ₁₀ +S ₁₁	244
52	<i>E</i>	S ₇ +S ₁₁	235	<i>E</i>	S ₇ +S ₁₁	221	<i>E</i>	S ₁₀ +S ₁₁	225	<i>E</i>	S ₁₀ +S ₁₁	222
53	<i>E</i>	S ₁₁ +S ₇	223	<i>B</i> ₁	S ₉	200	<i>B</i> ₁	S ₉	196	<i>B</i> ₁	S ₉	196
54	<i>E</i>	S ₁₀ +S ₁₁	217	<i>E</i>	S ₁₀ +S ₁₁	192	<i>E</i>	S ₁₀ +S ₁₁	189	<i>E</i>	S ₁₀ +S ₁₁	184
55	<i>B</i> ₁	S ₉	190	<i>E</i>	S ₁₀ +S ₁₁	167	<i>E</i>	S ₁₀ +S ₁₁	171	<i>E</i>	S ₁₀ +S ₁₁	163
56	<i>E</i>	S ₁₀ +S ₁₁	181	<i>E</i>	S ₁₀ +S ₁₁	152	<i>B</i> ₂	S ₆	153	<i>E</i>	S ₁₀ +S ₁₁	149
57	<i>B</i> ₂	S ₆	158	<i>E</i>	S ₁₀ +S ₁₁	143	<i>B</i> ₂	S ₆	137	<i>B</i> ₂	S ₆	135
58	<i>E</i>	S ₁₀ +S ₁₁	136	<i>E</i>	S ₁₀ +S ₁₁	127	<i>E</i>	S ₁₀ +S ₁₁	128	<i>E</i>	S ₁₀ +S ₁₁	123
59	<i>E</i>	S ₁₀ +S ₁₁	120	<i>E</i>	S ₁₀ +S ₁₁	103	<i>E</i>	S ₁₀ +S ₁₁	117	<i>E</i>	S ₁₀ +S ₁₁	111
60	<i>E</i>	S ₁₀ +S ₁₁	51	<i>E</i>	S ₁₀ +S ₁₁	43	<i>E</i>	S ₁₀ +S ₁₁	21	<i>E</i>	S ₁₀ +S ₁₁	29

Variations in other skeletal modes (Cr–N stretching and angle bending on the central metal atom) were observed but the shifts were not distinctly regular along the series X = F, Cl, Br, and I (Table IV). A plausible explanation might lie in the fact that skeletal vibrations in [Cr(NH₃)₅X]²⁺ are affected not only by the mass of the atom X, but also through at least two additional phenomena: a) by the capacity of X to produce a redistribution of electron density on ammine ligands through *d*-orbitals in a mechanism commonly referred to as *trans*-influence (Subsection: Modeling the *trans*-influence of X), and b) through intramolecular steric interactions that depend on the size of X.

Concerning the results listed in Table IV, it should be emphasized that *C*_{4v} symmetry labels, as well as the symmetry coordinates derived in the *C*_{4v} point group, were used to describe the low-frequency skeletal vibrations. As the present CFF calculations were performed on the complete 22-atom structure with full relaxation of all internal coordinates (*i.e.*, without any symmetry constraint), the present vibrational analysis pertains, in a strict sense, to [Cr(NH₃)₅X]²⁺ structures of lower (or at most *C*_s) symmetry. Consequently, a significant coupling in potential energy distribution (PED) was to be expected, and for this reason, only a few principal PED³⁹ contributions were shown in Table IV for each calculated vibrational frequency. The most noteworthy is the strong coupling of ammine torsions with N–Cr–N bending modes of the CrN₅X skeleton (not shown in Table IV, but clearly evident in computer animations of molecular vibrations,^{40,41} available from the authors upon request).

Modeling the trans-influence of X

It is noteworthy that the RESP program⁴ used in this work offers a straightforward and very convenient way to control the averaging of atomic charges over stereochemically equivalent atoms. This feature helped in the demarcation of axial from equatorial ammine nitrogens, where the difference in *q*(N) resulted from the *trans*-influence of the X atom in [Cr(NH₃)₅X]²⁺.

The *trans*-influence of X in $[\text{Cr}(\text{NH}_3)_5\text{X}]^{2+}$ is expected to manifest itself through elongation of the axial Cr–NH₃ bond, and concomitant lowering of its Cr–N stretching frequency. Both phenomena were noted in crystallographic and spectroscopic studies on octahedral complexes. The present CFF modeling of $[\text{Cr}(\text{NH}_3)_5\text{X}]^{2+}$ with VOFF established a lengthening of Cr–N bond *trans* to the halogenido ligand (*cf.* Fig. 1) for X = Cl, Br, and I on average by 0.011(5) Å in geometry optimization with RESP charges (obtained from ROHF computations using the cc-pVTZ basis set for Cr) while keeping all FF parameters and functions involving all N ligator the same. The *trans*-influence turned out to be unexpectedly weak in the case of $[\text{Cr}(\text{NH}_3)_5\text{F}]^{2+}$. These results are in qualitative agreement with the fact that the Cr–NH₃ bond *trans* to X is lengthened on average by 0.03 Å with respect to other Cr–NH₃ bonds in 57 crystal structures containing 161 Cr–NH₃ bonds retrieved from the most recent CSD,⁴² as well as with the recent findings of Shibahara, Akashi *et al.* on pentaaminenitrosylchromium(III) complexes exhibiting a particularly strong *trans*-influence of the NO

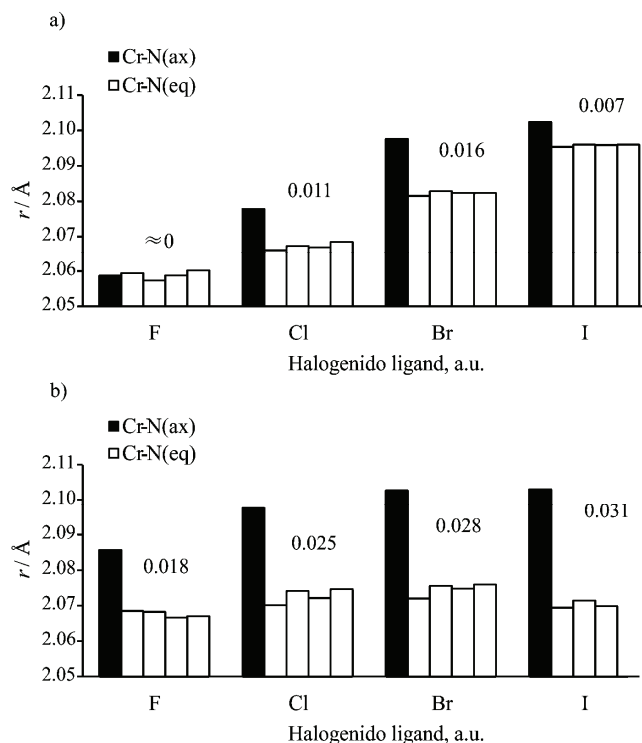


Fig. 1 Bond lengths (Å) for Cr–N^{ax} (*trans* to X) and Cr–N^{eq} in $[\text{Cr}(\text{NH}_3)_5\text{X}]^{2+}$ calculated with (a) CFF modeling and (b) DFT. DFT results were obtained with S-VWN/6-31+G(d). The values shown above the bars represent Δr_e , the difference between r_e^{trans} and the mean value of the four r_e^{cis} distances, which could be taken as a measure of the extent of *trans*-influence.

ligand.^{43–46} Furthermore, in a broader sense, the present results are in certain conformity with the current views on ligand ordering based on their *trans*-influence in square-planar metal complexes.⁴⁷

Differences in Cr–N bond lengths, as well as differences in their vibrations, are expected due to the presence of halogenido ligands and their *trans*-influence. Namely, as the axial Cr–N bonds in all molecules are shorter compared to equatorial ones, according to the general rule (shorter the bond – the larger the force constant – the greater the value of the wavenumber or vibration), the vibrations of Cr–N^{eq} bonds should have higher values compared to those of Cr–N^{ax} vibrations. If the individual contributions to the Cr–N vibrations are considered, the mentioned regularity is evident. The first calculated Cr–N vibrations (at the highest values of wavenumbers) originate exclusively from the equatorial Cr–N bonds, while the vibrations of the axial Cr–N bonds occur at lower values. For molecule [Cr(NH₃)₅F]²⁺, the frequency at 474 cm^{−1} has a dominant PED contribution of Cr–N^{eq} bonds, while the frequency at 387 cm^{−1} has dominant PED contribution of the Cr–N^{ax} bond (Table III). The frequency at 469 cm^{−1} originates only from vibrations of the equatorial Cr–N bonds of [Cr(NH₃)₅Cl]²⁺, but the vibrations of axial Cr–N occur at 448 cm^{−1}. The first calculated Cr–N vibration of the complex [Cr(NH₃)₅Br]²⁺ at 470 cm^{−1} belongs to Cr–N^{eq} bonds, while Cr–N^{ax} bonds contribute to the second frequency at 449 cm^{−1}. Finally, for the molecule [Cr(NH₃)₅I]²⁺, the calculated frequency at 469 cm^{−1} includes only vibrations of Cr–N^{eq} bonds, while frequency at 450 cm^{−1} has the highest contribution of vibrations of the Cr–N^{ax} bond.

Owing to the fact that structural data on [Cr(NH₃)₅F]²⁺ are not available, and that most of the published crystal structures of [Cr(NH₃)₅X]²⁺ with other halogenido ligands do not offer sufficiently conclusive evidence on the *trans*-influence of X, additional DFT calculations were performed for the whole series. First, it was observed that the recommended B3LYP functional⁴⁶ produces expected trends but yields excessively large metal–ligand distances. However, acceptable bond lengths were obtained with the S-VWN functional with basis sets as cited in the Section Methodology. The latter DFT results indeed revealed *trans*-influence for all four halogenido ligands, with reasonable Δr_e values ($r_e^{\text{trans}} - r_e^{\text{cis}}$) for the Cr–N bonds, substantiating the trends resulting from the CFF modeling to the greatest extent possible in any comparison of QM and MM approaches.

The expected lowering of $\nu(\text{Cr–N}^{\text{ax}})$ is more difficult to distinguish due to admixture of $\nu(\text{Cr–X})$ and $\nu(\text{Cr–N}^{\text{ax}})$ in both S₄ and S₅ symmetry coordinates (Table IV and Fig. S-2 of the Supplementary material) and additional coupling with $\nu_s(\text{Cr–N}^{\text{eq}})$ (S₁), which was apparent in CFF modeling. It should be noted that this approach to model the *trans*-influence falls entirely within the force field (molecular mechanics) paradigm, *i.e.*, parametric representation of the potential

energy surface allowing for second-order stereochemical phenomena, and therefore does not propose an explanation for the origin of the *trans*-influence. As such, or with possible refinements or extensions (of which there are several), it may have some conceptual resemblance to the modeling of the *trans*-influence with VALBOND-TRANS force field.^{8,48}

CONCLUSIONS

By extending the recently proposed scheme¹ for the derivation of partial atomic charges for chromium(III) complexes from QM computed MEP using the RESP procedure,² onto the mixed halogenido–ammine complexes with F, Cl, Br, and I ligands, and using such charges together with the vibrationally optimized force field (VOFF) for coordination compounds,¹⁰ a reliable and physically realistic model was built, which was capable of reproducing experimental structures and vibrational frequencies in a consistent way throughout the series of $[\text{Cr}(\text{NH}_3)_{6-n}(\text{X})_n]^{(3-n)+}$ species ($n = 1$; X = F, Cl, Br, I). The results for the other series ($n > 1$), not shown here due to the lack of experimental data, appear to be consistent with the ones presented.

In the course of this study it was necessary to define reference Cr–X bond distances, which were derived from a statistical analysis of the data from the CSD base that contained a 10-fold increase in measured Cr–X distances (a total of 254 relevant values) with respect to the 24 values used in the previous such compilation.³⁰

The calculated vibrational frequencies with the present VOFF were in accordance with available experimental data over the whole frequency range (3500–100 cm⁻¹). In particular, the low-frequency skeletal vibrations were reassigned in the C_{4v} point group of the CrN₅X core, their shifts across the series (X = F, Cl, Br, I) were elucidated, and the presence of a strong coupling between some skeletal bending modes and torsional motion of ammine ligands was observed in the present zero torsional barrier approximation.

Finally, differences in the RESP derived partial atomic charges between the axial and equatorial ammine ligands in $[\text{Cr}(\text{NH}_3)_5\text{X}]^{2+}$, presumably due to second-order electronic effects, seem to offer a simple and straightforward way to incorporate *trans*-influence in force field modeling of coordination compounds, which manifested itself in the elongation of metal–ligand bonds in an expected way and to a plausible extent.

SUPPLEMENTARY MATERIAL

Additional VOFF parameters for $[\text{Cr}(\text{NH}_3)_5\text{X}]^{2+}$, the distribution of the Cr–X bond distances, a review of published atomic charges, the symmetry coordinates of $[\text{Cr}(\text{NH}_3)_5\text{X}]^{2+}$, the distribution of the symmetry vibrations and DFT calculated vibrational frequencies are available electronically from <http://www.shd.org.rs/JSCS/>, or from the corresponding author on request.

Acknowledgements. Financial support from the Serbian Ministry of Education, Science and Technological Development of the Republic of Serbia through Grant No. 172035 is gratefully acknowledged. We thank the Centre for Molecular and Biomolecular Informatics, Radboud University Nijmegen, for access to the Cambridge Crystal Structure Database (CSD).

И З В О Д

РАЗВИЈАЊЕ НОВОГ СКУПА ПАРАМЕТАРА ПОЉА СИЛА ЗА ХАЛОГЕНИДО-
-АММИНСКЕ КОМПЛЕКСЕ ХРОМА(III): МОДЕЛИРАЊЕ *trans*-УТИЦАЈА
ХАЛОГЕНИДО ЛИГАНАДА

ИВАНА ЂОРЂЕВИЋ¹, СОЊА ГРУБИШИЋ¹, МИЛОШ МИЛЧИЋ² И СВЕТОЗАР НИКЕТИЋ¹

¹Центар за хемију, ИХТМ, Универзитет у Београду, Нђошева 12, 11001 Београд и ²Хемијски
факултет, Универзитет у Београду, Студентски трг 16, 11001 Београд

На серији октаедарских халогенидо-амминских комплекса хрома(III) приказан је нов приступ за моделирање *trans*-утицаја, користећи парцијална атомска наелектрисања изведене фитовањем из молекулског електростатичког потенцијала применом RESP методе. RESP наелектрисања заједно с приказаним вибрационо оптимизованим пољем сила објашњавају феномене другог реда, поспешују моделирање и асигнују скелетних вибрација, и репродукују правилности у вибрационим помацима у низу халогенидо лиганада F, Cl, Br и I. Поред тога, дата је статистичка анализа за дужине Cr-халоген веза у кристалним структурама из Cambridge банке кристалографских података (CSD).

(Примљено 3. септембра, ревидирано 26. октобра, прихваћено 27. октобра 2014)

REFERENCES

- I. S. Djordjević, S. R. Niketić, *Comput. Theor. Chem.* **1001** (2012) 20
- F.-Y. Dupradeau, A. Pigache, T. Zaffran, C. Savineau, R. Lelong, N. Grivel, D. Lelong, W. Rosanski, P. Cieplak, *Phys. Chem. Chem. Phys.* **12** (2010) 7821
- F.-Y. Dupradeau, A. Pigache, T. Zaffran, P. Cieplak, *R.E.D. User's Manual and Tutorial*, version 2.0, <http://q4md-forcefieldtools.org/RED/RED-II.pdf> (accessed in 2005)
- RESP standalone*, version 2.3, <http://q4md-forcefieldtools.org> (accessed in 2011)
- K. B. Yatsimirskii, *Pure Appl. Chem.* **49** (1977) 115
- J. Gažo, R. Boča, E. Jóna, M. Kabešová, Ľ. Macášková, J. Šima, *Coord. Chem. Rev.* **43** (1982) 87
- A. E. Anastasi, R. J. Deeth, *J. Chem. Theory Comput.* **5** (2009) 2339
- I. Tubert-Brohman, M. Schmid, M. Meuwly, *J. Chem. Theory Comput.* **5** (2009) 530
- C. I. Bayly, P. Cieplak, W. D. Cornell, P. A. Kollman, *J. Phys. Chem.* **97** (1993) 10269
- a) J.-H. Choi, S. R. Niketić, I. S. Djordjević, W. Clegg, R. W. Harrington, *J. Mol. Model.* **18** (2012) 2135; b) S. Grubisić, S. R. Niketić, D. D. Radanović, U. Rychlewska, B. Warzajtis, *Polyhedron* **24** (2005) 1701
- M. Schmidt, K. K. Baldridge, J. A. Boatz, S. Elbert, M. Gordon, J. H. Jenson, S. Koeski, N. Matsunaga, K. A. Nguyen, S. J. Su, T. L. Windus, M. Dupuis, J. A. Montgomery, *J. Comput. Chem.* **14** (1993) 1347
- A. K. Rappé, T. A. Smedley, W. A. Goddard III, *J. Phys. Chem.* **85** (1981) 2607
- W. J. Stevens, M. Krauss, H. Basch, P. G. Jasien, *Can. J. Chem.* **70** (1992) 612
- T. R. Cundari, W. J. Stevens, *J. Chem. Phys.* **98** (1993) 5555
- N. B. Balabanov, K. A. Peterson, *J. Chem. Phys.* **123** (2005) 064107-1

16. M. M. Franel, W. J. Pietro, W. J. Hehre, J. S. Binkley, M. S. Gordon, D. J. DeFrees, J. A. Pople, *J. Chem. Phys.* **77** (1982) 3654
17. L. A. Curtiss, M. P. McGrath, J. P. Blaudeau, N. E. Davis, R. C. Binning Jr., L. Radom, *J. Chem. Phys.* **103** (1995) 6104
18. M. N. Glukhovtsev, A. Pross, M. P. McGrath, L. Radom, *J. Chem. Phys.* **103** (1995) 1878
19. W. J. Hehre, R. Ditchfield, J. A. Pople, *J. Chem. Phys.* **56** (1972) 2257
20. Y. Duan, C. Wu, S. Chowdhur, M. Lee, G. Xiong, W. Zhang, R. Yang, P. Cieplak, R. Luo, T. Lee, J. Caldwell, J. Wang, P. Kollman, *J. Comput. Chem.* **24** (2003) 1999
21. D. L. Mobley, É. Dumont, J. D. Chodera, K. A. Dill, *J. Phys. Chem B* **111** (2007) 2242
22. S. Patel, A. MacKerell Jr., *J. Comput. Chem.* **25** (2004) 1504
23. Gaussian 09, Revision D.01, Gaussian, Inc., Wallingford, CT, 2009
24. C. Lee, W. Yang, R. G. Parr, *Phys. Rev., B* **37** (1988) 785
25. A. D. Becke, *J. Chem. Phys.* **98** (1993) 1372
26. P. J. Hay, W. R. Wadt, *J. Chem. Phys.* **82** (1985) 270
27. S. Vosko, L. Wilk, M. Nusair, *Can. J. Phys.* **58** (1980) 1200
28. J. C. Slater, *Phys. Rev.* **81** (1951) 358
29. P. A. M. Dirac, *Proc. R. Soc. London, Ser. A* **123** (1929) 714
30. A. G. Orpen, L. Brammer, F. H. Allen, O. Kennard, D. G. Watson, R. Taylor, *J. Chem. Soc., Dalton Trans.* **12** (1989) S1
31. S. Lifson, in *Dynamic Aspects of Conformational Changes in Biological Macromolecules*, C. Sadron, Ed., D. Reidel, Dordrecht, 1973, p. 421
32. S. Lifson, in *Supramolecular Structure and Function*, G. Pifat, J. H. Herak, Eds., Springer, New York, 1983, p. 1
33. K. Kuchitsu, in *Proceedings of Critical Evaluation of Chemical and Physical Structural Information*, Dartmouth College, Washington DC, 1974, p. 132
34. J. R. Ferraro, J. S. Ziomek, *Introductory Group Theory and Its Application to Molecular Structure*, Plenum Press, New York, 1975
35. H. H. Schmidtke, M. Rosner, *Inorg. Chem.* **28** (1989) 2510
36. N. Tanaka, M. Kamada, J. Fujita, E. Kyuno, *Bull. Chem. Soc. Jpn.* **37** (1964) 222
37. S. Lifson, A. Warshel, *J. Chem. Phys.* **49** (1968) 5116
38. A. Warshel, M. Levitt, S. Lifson, *J. Mol. Spectrosc.* **33** (1970) 84
39. S. Califano, *Vibrational States*, Wiley, London, 1976
40. MOLEKEL 4.3, Swiss Center for Scientific Computation, Manno, Switzerland, 2000
41. S. Portmann, H. P. Lüthi, *Chimia* **54** (2000) 766
42. S. R. Niketić, unpublished analysis of CSD data, 2013
43. H. Akashi, M. Mori, T. Shibahara, *Acta Crystallogr., E* **57** (2001) i75
44. H. Akashi, M. Mori, T. Shibahara, *Inorg. Chim. Acta* **331** (2002) 290
45. H. Akashi, T. Yamauchi, T. Shibahara, *Inorg. Chim. Acta* **357** (2004) 325
46. T. Shibahara, H. Akashi, M. Asano, K. Wakamatsu, K. Nishimoto, M. Mori, *Inorg. Chem. Commun.* **4** (2001) 413
47. F. A. Weinhold, C. R. Landis, *Valency and Bonding: A Natural Bond Orbital Donor-Acceptor Perspective*, Cambridge University Press, New York, 2005
48. J. Huang, M. Devereux, F. Hofmann, M. Meuwly, in *Computational Organometallic Chemistry*, O. Wiest, Y. Wu, Eds., Springer, Heidelberg, 2012, p. 19.